TABLE 1

MODEL CHARACTERISTICS

Model	Θ [°]	v_j [km s^{-1}]	$\dot{M}_j$ [$M_\odot$ s^{-1}]	v_a [km s^{-1}]	n_a [cm^{-3}]	R_0 [10^{17} cm]	$d_c{}^r/(R_0\tan\Theta)$	$d_c{}^f/(R_0\tan\Theta)$	Resolution
1	10	200	1.00×10^{-10}	125	0.044	2.97	402.4	11.9	lr,mr,hr
2	20	200	3.97×10^{-10}	125	0.044	2.97	194.9	5.7	mr
3	30	200	8.82×10^{-10}	125	0.044	2.97	122.9	3.6	mr
4	10	200	1.00×10^{-9}	125	0.044	9.39	127.2	3.7	mr
5	20	200	3.97×10^{-9}	125	0.044	9.39	61.6	1.8	mr
6	30	200	8.82×10^{-9}	125	0.044	9.39	38.9	1.1	mr
7	10	40	1.00×10^{-10}	100	1.0	3.48	0.28	1.3	mr

mass loss rate and opening angle) has the broadest flow. Independently of the $\dot{M}_j$ and Θ values, all three models coincide with the theoretical stagnation point ($R_0 = 2.97\times10^{17}$ cm), and they also have tails with the same basic morphology. It is clear that the numerical simulations produce broad interaction regions, which are a direct result of the fact that the post-shock cooling distances ($d_c{}^r$, and $d_c{}^f$, see Table 1) are not small compared to the width of the flows. We find that the thin layer analytic solution lies along a line dividing the computed flows into two regions: an internal low-density, hot region (corresponding to the jet cocoon) and a high-density external, cold region (corresponding to the shocked, streaming ambient medium).

The fact that the cooling distances are large compared to the cross section of the jet indicates that the flows are non-radiative. In this case it is remarkable that the analytical solution does successfully divide the hot/low-density from the cold/high-density regions. This is not necessarily expected, as the analytical model assumes that the material is well mixed in a thin layer, which would arise more naturally in radiative flows (where cooling occurs in a small region).

The density and temperature stratifications (at $t = 5\times10^3$ yr) for models 4–6 are shown in Figure 7. These models, with mass loss rates one order of magnitude larger than those of the first three models ($\sim10^{-9}$ $M_\odot$ s^{-1}, for details see Table 1) have smaller cooling distances than models 1–3; however, they are still in the non-radiative regime. The three models roughly match the analytically derived stagnation point ($R_0 = 9.39\times10^{17}$ cm), and produce broader flows for larger values of the opening angle Θ.

In order to check how well the numerical simulations reproduce the theoretical stagnation point in the thin shell analytical solution from § 2, we show

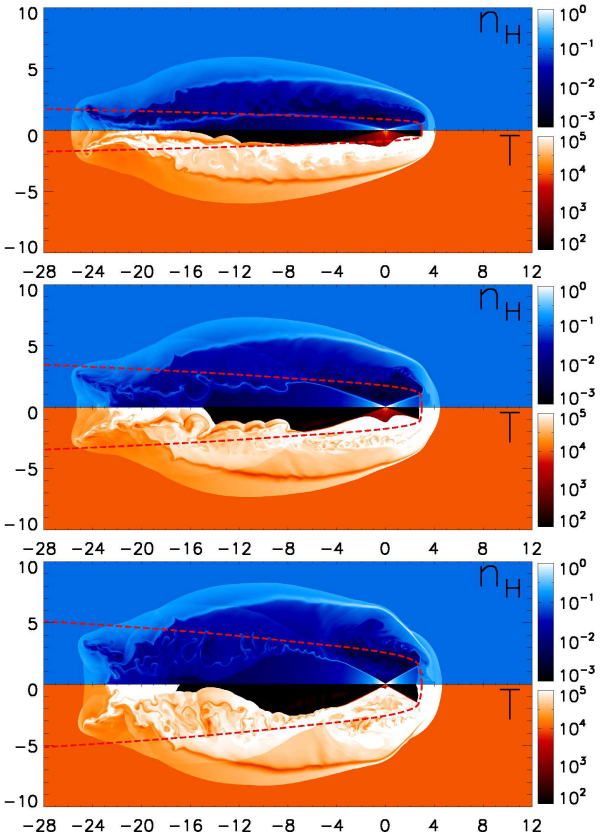

Fig. 6. Density stratifications (color scale given in cm^{-3}, blue panels); and temperature (color scale given in K, orange panels). Top, middle and bottom figures correspond to models 1, 2 and 3 (respectively). The integration time is $t = 5\times10^3$ yrs (top). The axes are labeled in units of 10^{17} cm. The broken line delimits the analytic solution proposed in § 2. The color figure can be viewed online.

a zoom of the density structures of the jet heads for all models in Figures 8–9. We find that a steady state is reached (with small discrepancies, more evident in models 4–7, Figure 9), with a shock structure approximately centered on the stagnation radius R_0